THE ROLE OF STRETCH-INDUCED MECHANOTRANSDUCTION IN THE AIRWAY EPITHELIUM OF THE DEVELOPING LUNG

by

Mercedes Dayan

A thesis submitted to the Faculty of the University of Delaware in partial fulfillment of the requirements for the degree of Honors Bachelor of Science in Neuroscience with Distinction

Spring 2019

THE ROLE OF STRETCH-INDUCED MECHANOTRANSDUCTION IN THE AIRWAY EPITHELIUM OF THE DEVELOPING LUNG

by

Mercedes Dayan

Approved:

Jason Gleghorn, Ph.D.
Professor in charge of thesis on behalf of the Advisory Committee

Approved: _____

Randall L. Duncan, Ph.D
Committee member from the Department of Biological Sciences

Approved: _____

Carlton R. Cooper, Ph.D
Committee member from the Board of Senior Thesis Readers

Approved: _____

Earl Lee II, Ph.D.
Deputy Faculty Director, University Honors Program

ACKNOWLEDGMENTS

Thank you to Dr. Jason Gleghorn, for the opportunity to work in your lab with an incredibly intelligent group of people and thank you for all the guidance throughout this process. Thank you for your support and advice in all aspects of my undergraduate career. You helped me to become a stronger student and researcher. To all the graduate students for their support, and especially Rachel Gilbert for being a true friend and incredible resource for my thesis. Thank you for going above and beyond for me. Thank you for teaching me numerous laboratory skills and helping me to work through all the obstacles in my project. To the University of Delaware Research Program for making undergraduate research possible and for all of the funding that they have contributed. Lastly, thank you to my family for their love and support.

TABLE OF CONTENTS

LIST OF TABLES

LIST OF FIGURES

ABSTRACT

This study provides a quantitative methodology to measure and apply controlled strain to a cellular system as a means of studying embryonic lung development. The development of the type of model it provides will enable researchers to obtain new insight on lung mechanotransduction pathways and to determine the effects of various parameters of strain on developing lungs. An acrylic strain device was used and calibrated to deliver repeatable strain to the MLE-12 cell line.

The device was coated with fibronectin for one hour, which enabled cell adhesion. Cells were then seeded and cultured overnight such that they reached 80-90% confluency prior to the experiment. A novel LabView program was developed to operate the strain device and enabled control of parameters including frequency of stretch and amount of stretch to be applied. Assays were optimized for the MLE-12 cell line including: Fluo-8AM and K-Ras pulldown assay. Whole lung explants were analyzed to determined baseline frequency of lung contractions and kymographs were obtained. Cells were stretched at a frequency of 3.30 with a duty cycle of 3.33%, which corresponds to a 10 second stretch, once every 5 minutes. Cells were analyzed for proliferation with an Edu Assay Kit. Analysis was done using a novel MatLab script created by our lab and modified. A GCamp cell line was created in order to visualize calcium flux in real time during stretch. Effects were analyzed using ImageJ.

Proliferation data did not follow the trends suggested by the literature and decreasing background fluorescence skewed fluorescence measurements in the GCamp dataset. Deviations from suggested trends were likely due to flaws in the

device itself, as shown in calibration data. Overall, this study provides a methodology for studying lung development with the creation of a novel strain device. The methods described in this study could help to guide future experiments that will enable researchers to elucidate pathways of mechanotransduction in the developing lung and develop targeted therapeutics for developmental pulmonary diseases.

Chapter 1

INTRODUCTION

1.1 Developmental Pulmonary Disease

Congenital Diaphragmatic Hernia (CDH) is a developmental pulmonary disease which is characterized by decreased lung growth and can lead to fatal pulmonary hypertension. It affects 1 in every 2500 live births, making it one of the most prevalent and lethal lung development abnormalities.[1]

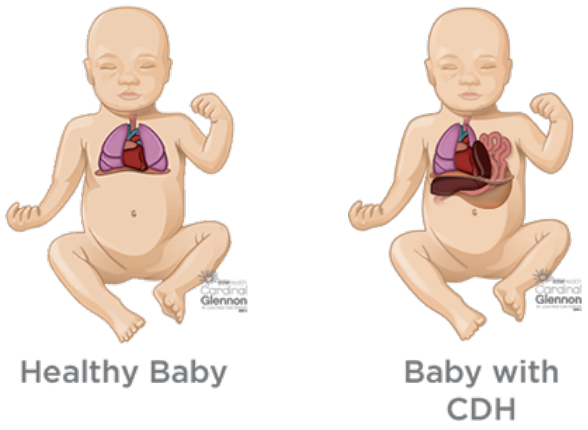

Figure 1: Babies with CDH exhibit underdeveloped lungs in comparison to their healthy counterparts.[2]

One of the fundamental aspects of CDH that leads to poor lung development is altered pressure dynamics due to malformation of the diaphragm. The abdominal organs press into the chest cavity leading to compression of the lungs. This results in pulmonary

hypoplasia, or underbranched lungs. However, the signaling mechanisms that cause these changes remain unknown. The present study aims to investigate the signaling pathway through which pressure-mediated changes occur. It specifically studies embryonic mouse lung cells using an immortalized cell line (MLE-12) and uses a 3D culture model to examine varying pressure conditions.

1.2 Lung Pressure Dynamics and Morphogenesis

In healthy developing lungs, pressure in maintained through both fluid and breathing movements within the fetus[8]. However, since CDH leads to compression of the lungs, this results in the disruption of the lungs' physical environment and altered pressure dynamics. Empirically, pressure has been shown to play a role in physiological lung development[3]. Specifically, as seen in figure 2, increased pressure in the airway epithelium leads to increased branching and growth[4].

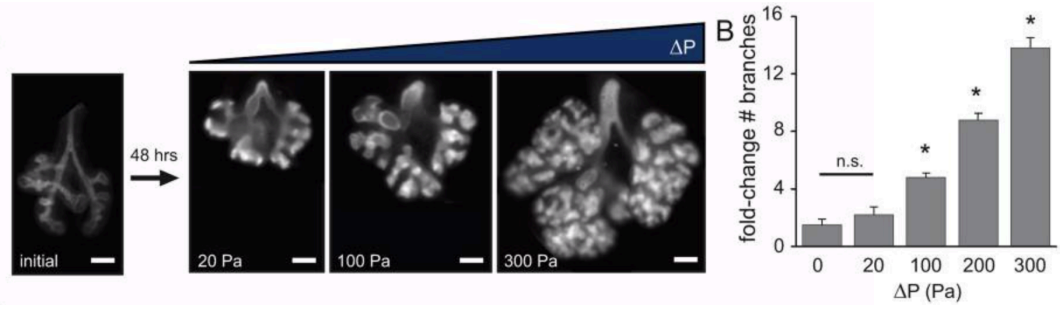

Figure 2: Lung growth measured in number of branches during different pressure conditions (from Nelson et al., 2017).

1.3 Peristaltic Contractions and Branching Morphogenesis

Lung branching is synchronized and regulated by transmural pressure[4]. There is also a direct relationship between pressure and frequency of peristaltic contraction[4]. Additionally, studies have shown that there is a correlation between peristaltic lung contraction and lung growth[9]. For example, *ex vivo* models have demonstrated that inhibition of peristaltic contractions are associated with a concurrent inhibition of lung growth. Nifidipine, an L-type calcium channel blocker, inhibits contractions, resulting in decreased branching[4].

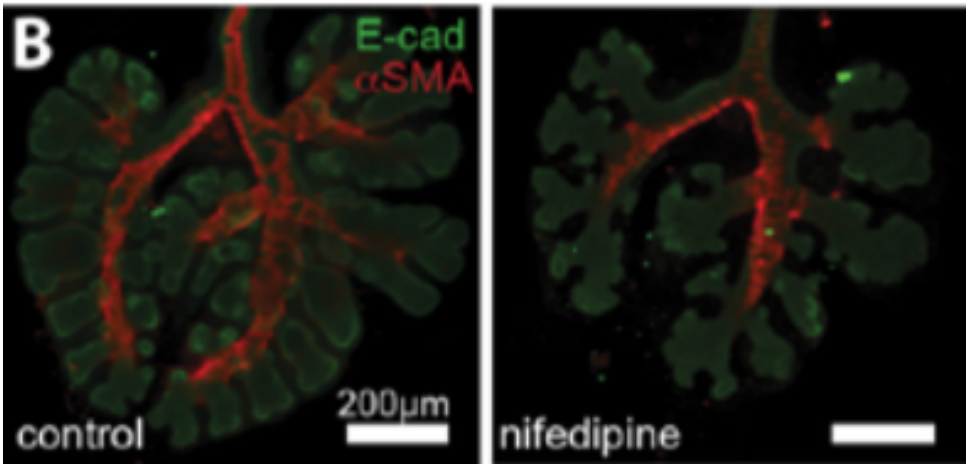

Figure 3: Nifedipine-induced hypoplastic lungs vs. healthy control lungs stained for E-cadherin and smooth muscle actin (modified from Nelson et al., 2017).

Hypoplastic (underdeveloped) lungs induced by nitrofen exposure, another agent that halts peristaltic contractions, also show deficits in lung growth. These lungs exhibit not only decreased budding, but also decreased numbers of contractions[7].

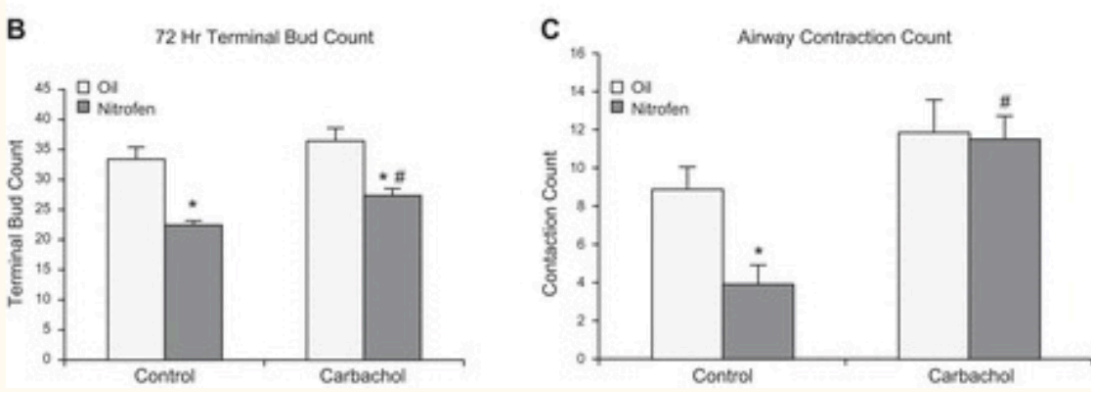

Figure 4: Difference in bud count and airway contraction in "normal" vs. hypoplastic lungs (modified from Rhodes et al. 2015).

Because of these discoveries and other work in the field, it is thought that peristaltic contractions are coupled with lung growth through a mechanism involving epithelial stretch[4]. Studies have found that strain applied to rat lung cells enhanced growth and development of a three-dimensional configuration[6].

Thus far, the connection between the role of smooth muscle contractions and branching in the airway epithelium remains unclear. However, a likely mechanism is that stretch in the epithelium, induced by peristalsis, leads to the cellular signaling patterns that ultimately promote proliferation. Additional branching would require increased proliferation. In a study of fetal rat epithelium, cells that were stretched showed increased proliferation and DNA synthesis[6]. Additionally, stretch-induced proliferation is found in multiple other organ systems including the kidney, bladder, prostate, and heart[28, 29, 30, 31]. This highlights the key role of pressure and stretch in organ development and cellular proliferation.

1.4 Determining the Molecular Mediators of Epithelial Mechanotransduction

Since CDH is caused by a variety of environmental and genetic components, it is complicated to find a specific signaling pathway that can be targeted for treatments. The mechanism for lung peristalsis is still unclear, but studies point to ion channels as possible mediators of this action. Furthermore, calcium release seems to be involved[10,11]. One study showed that fetal calcium regulates branching morphogenesis in developing mouse and human lung[14]. Another study showed that as little as one stretch could result in calcium mobilization in lung epithelial cells[32]. TRPV4, calmodulin and Ras have also been suggested to be important to mechanotransduction pathways.

1.4.1 Role of TRPV4

TRPV4, a mechanosensitive calcium cation channel, has been implicated as a potential regulator of peristalsis[10]. TRPV4 has been identified in adult lung tissue as well as fetal murine lung tissue throughout various developmental stages including E16, E17, E18, and E19 and in various parts of lung tissue including the epithelium and mesenchyme[12].

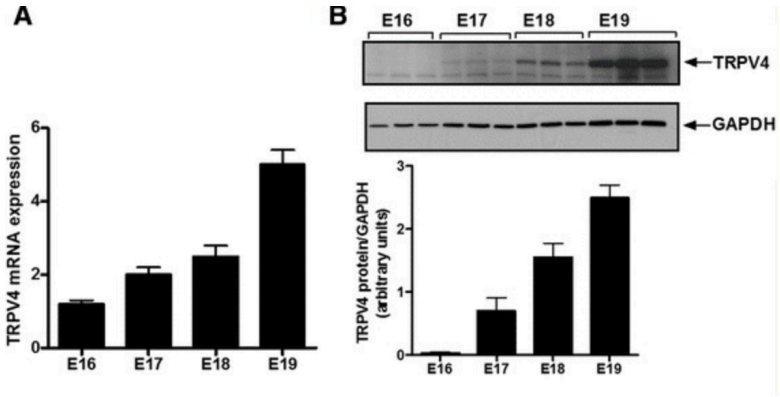

Figure 5: TRPV4 expression in fetal murine lung tissue during development (modified from Nayak et al., 2015).

Additionally, activation of TRPV4 with GSK101, a TRPV4 agonist, has been shown to accelerate lung branching in a murine mouse model, while GSK205, a TRPV4 antagonist has been shown to decrease this effect[13].

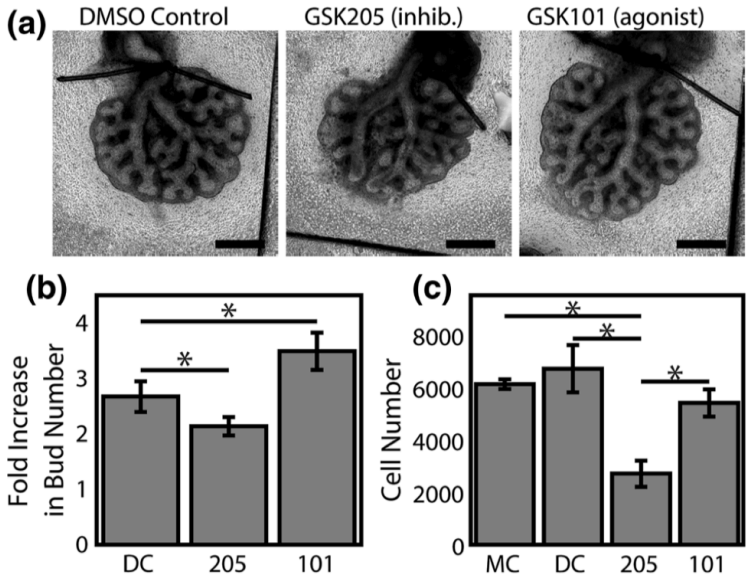

Figure 6: Effects of TRPV4 agonism and antagonism on lung explants' growth and on cell proliferation in MLE12 cells (from Morgan et al. 2018).

Furthermore, TRPV4 is involved in peristaltic contractions within the lung, as TRPV4 agonists increase contraction rate and antagonists decrease contraction rate[13].

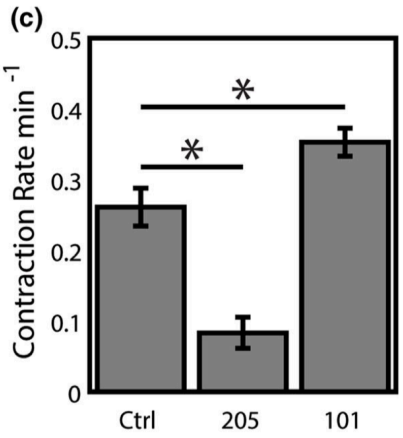

Figure 7: Rate of murine lung contraction of lungs isolated at E12.5 and exposed to GSK205 and GSK101 (modified from Morgan et al. 2018).

Overall, this data supports the role of TRPV4 as a potential mediator of the effects of pressure on the development of the lung.

1.4.2 Role of CaM and Ras

It is likely that the effects of calcium influx in the lung are mediated through the expression of CaM-dependent RasGRF (Ras Protein-Specific Guanine Nucleotide-Releasing Factor). RasGRF expression has been validated within the embryonic lung and is found in both isoforms RasGRF-1 and RasGRF-2[22,23]. This also coincides with the proposed signaling cascade, as RasGRF is primarily activated by calcium influx via the action of CaM (calmodulin)[21]. Furthermore, RasGRF promotes Ras activation of Rho GTPases and Ras[24,25]. RasGRF also regulates K-Ras activity, which makes it a

logical potential link between TRPV4 calcium influx and proliferation since K-Ras is known to have proliferative effects and has been highly studied in cancer biology.

1.4.3 Role of K-Ras

Studies have shown that K-Ras is crucial within fetal development, as K-Ras mutants result in embryonic lethality by E12[15]. Additionally, K-Ras is crucial within the lung because it is a key regulator of branching morphogenesis[16,17,18]. In one study, increasing K-Ras within the developing lung led to decreased alveolarization but increased branching[19]. In a different study, K-Ras mutants showed profound defects in lunch branching morphogenesis[20].

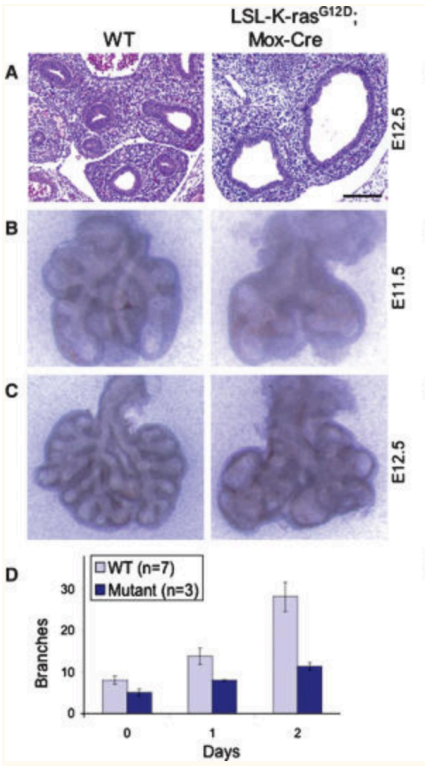

Figure 8: Comparison of wild-type and K-Ras mutant lungs throughout various stages of development (from Shaw et al. 2007).

Thus, these studies show that K-Ras is essential to proper lung development. K-Ras activation will be analyzed. The activated state is when K-Ras is bound to GTP. The inactivated state is K-Ras bound to GDP.

1.5 Limitations of Current Models

While other studies have sought to mimic epithelial stretch in vitro, the methods utilized were often outdated or expensive. One 1995 study employed a solenoid and sponge technique of stretching cells to determine rates of proliferation; however, pressure and time of stretch were arbitrarily selected and the amount of stretch applied was somewhat ambiguous[6]. Meanwhile numerous other studies rely on expensive systems to test the effects of equibiaxial strain on various cell types[25,26]. Finally, there are currently no studies that have investigated a pathway of mechanotransduction within the airway epithelium. Pressure-induced stretch is essential to the development of several different organs, such as: lungs, prostate, and bladder. The development of the proposed model can then be used to gain insight into additional signaling pathways of various biological systems at the cellular level.

1.6 Hypothesis and Specific Aims

I hypothesized that a potential developmental mechanotransduction signaling pathway dependent on stretch could rely on TRPV4 followed by calcium release and calmodulin activation, RasGRF activation, KRas activation, and ultimately proliferation. My first aim was to establish a way to accurately measure calcium in order to determine whether there is a connection between stretch, TRPV4, and KRas activation. My second aim was to establish a way to accurately measure KRas activation in order to determine whether stretch was leading to KRas activation. My

third aim was to determine baseline proliferation measurements with the novel device to further validate the model.

Chapter 2

METHODS

2.1 Creating a Device for Applying Cyclic Stretch in Vitro

We used a laser cut acrylic base for the device pillars. The device consists of a series of 9 pillars: 3 control, 3 small, and 3 large pillars arranged in a square pattern to ensure consistency of deformation. Subsequently, the PDMS housing for the cells is made by first cutting out the pattern of the device and punching 6mm round holes for the pillars. Thin PDMS membranes of 10um thickness are made using a spinner and then attached to the PDMS housing by oxygen plasma treatment to create a series of cell chambers.

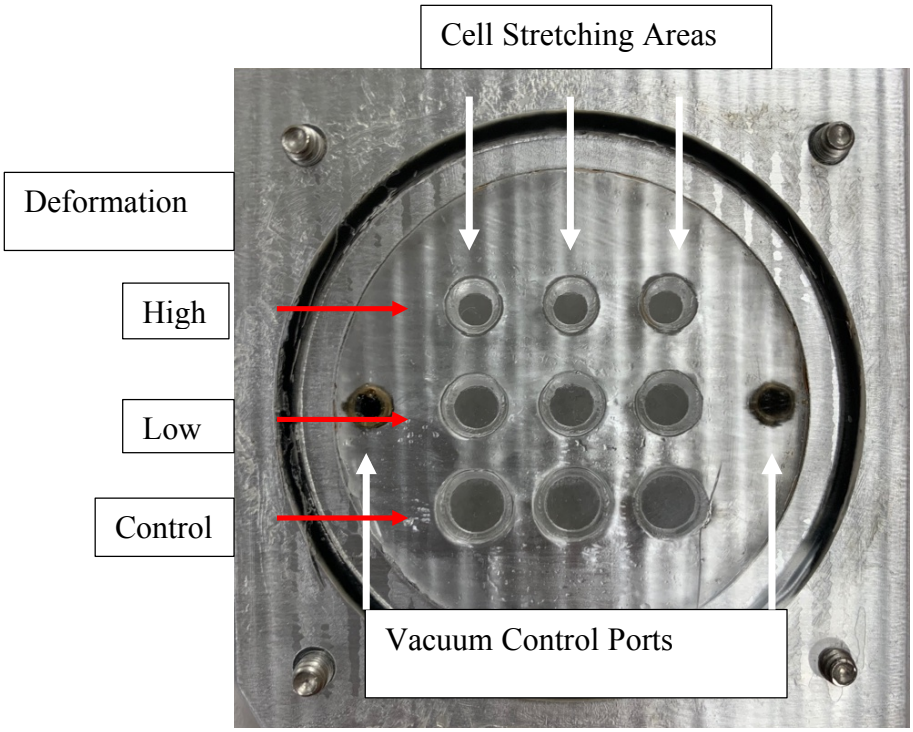

Figure 9: Acrylic device with PDMS on top for cell stretch.

When the vacuum is applied, the areas of thin PDMS on the cell chamber will deform across the pillars. The cell chambers are seeded with MLE-12 cells and the MLE-12 cells stretch as the PDMS membrane stretches.

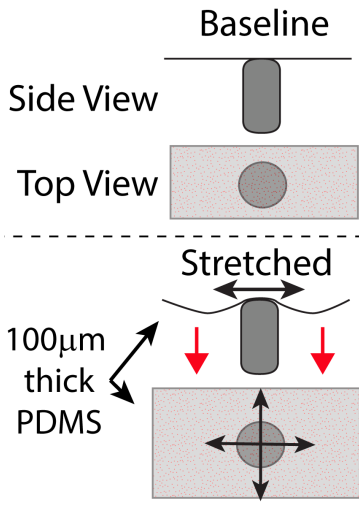

Figure 10: Schematic view of how pillars function to pull on PDMS membranes causing a deformation of the cells seeded on top.

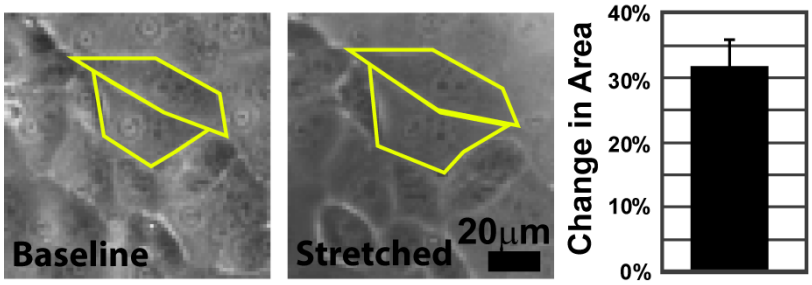

Figure 11: MLE12 cells being stretched with the above device.

2.2 Defining In Vivo Conditions

In order to determine what in vivo conditions are like, embryonic mouse lungs (E12.5) were cultured for 24 hours and lung contractions were recorded using kymographs. Analysis of preliminary data from our lab has shown a range of 6-13 contractions every 30 minutes, or 12-26 contractions per hour.

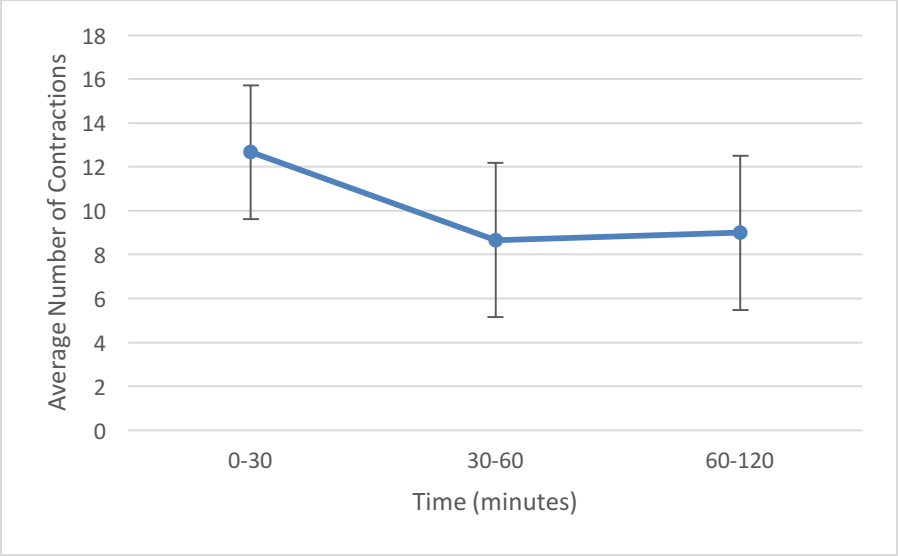

Figure 12: Average number of contractions of embryonic mouse lungs, as measured via kymograph analysis. Three lungs were averaged in each time point.

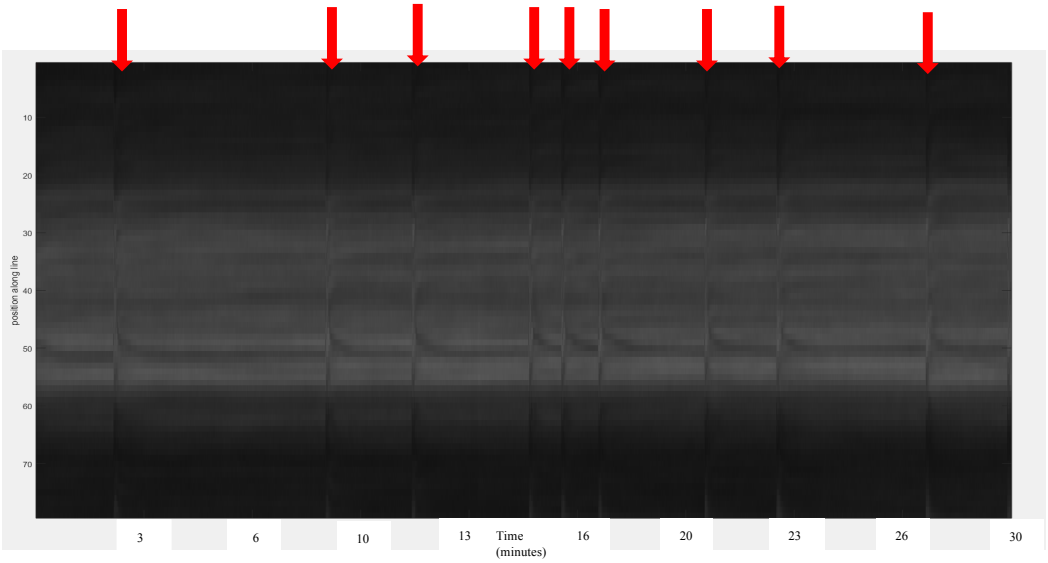

Figure 13: Sample kymograph, where each vertical line represents one contraction. Arrows mark contractions.

2.3 Utilizing In Vivo Analysis to Guide In Vitro Experiments

Due to the above mentioned data, the stretch conditions applied were: three hours total stretch time, frequency of 3.3mHz, and duty cycle of 3.30%. This would be approximately 1 stretch every 5 minutes, for a 10 second duration of stretch. The cyclic stretch was then applied for a total 3 hours. These parameters were applied using a LabView program designed to work with a vacuum, DAQ, and input and output ports within the device.

2.4 Optimizing Protocols for Assaying Components of Molecular Pathway

2.4.1 Proliferation Studies

Analysis of proliferation was preformed using a Click-iT EdU Assay Kit (Thermo). Edu is incorporated within DNA during DNA synthesis indicating which cells proliferated during the time of application. EdU (Component A), was diluted in media and after previously stretching for 2.5 hours, a 30 minute pulse was performed during the final 30 minutes of stretch. Following application of the EdU, cells were fixed with 4% PFA (paraformaldehyde) and rinsed with PBST (phosphate buffered saline with 0.5% tween). Then the cells were permeabilized using a 0.5% Triton-X100 solution. The Click-iT reaction was then performed using $CuSO_4$, DMSO, "Reagent F," diH_2O and the fluorophore (Alexa Fluor 647). This was incubated at room temperature, protected from light for 30 minutes. The reaction was then rinsed and cells were stained with DAPI.

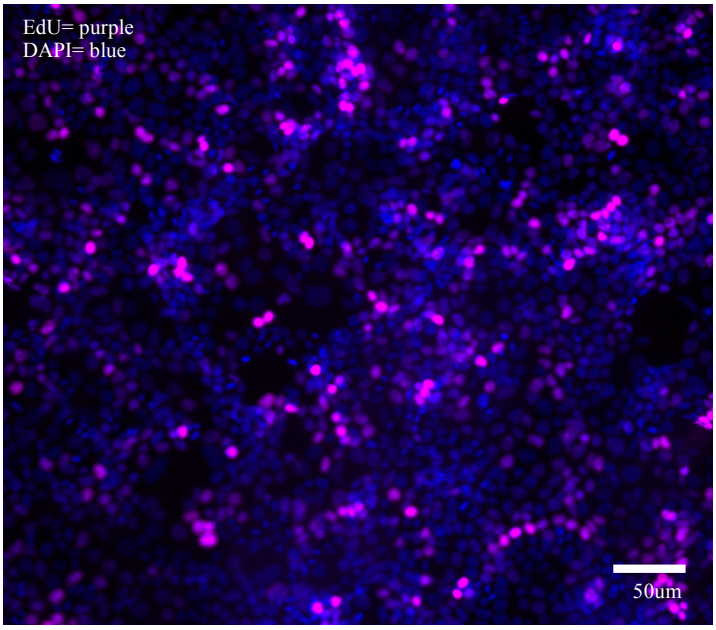

Figure 14: MLE12 cells after 30 minute EdU pulse and DAPI stain during the last 30 minutes of 3 hours of medium strain and DAPI counter stain.

2.4.1.1 Imaging Devices After Proliferation Assay

After staining, a 6mm punch was used to remove the thin PDMS membrane from each well of the cell chamber. This membrane was then flipped and mounted onto a glass coverslip using 2uL of gelvatol to allow for easier imaging.

2.4.2 Western Blotting and Pull-Down Assays

Western blotting is done to detect protein in a semi-quantitative way. Western blotting was performed to confirm the presence of K-Ras in MLE-12 cells and as a preliminary step for the pull-down assay. Western blotting was performed using whole cell MLE12 lysates separated on a 10%-12% gradient SDS/polyacrylamide gel and transferred ontowith nitrocellulose membranes. Membranes were blocked with milk and then incubated with anti-KRas rabbit monoclonal antibody. Femto was used for

chemi-luminescence detection and membranes were exposed for two minutes. After imaging for K-Ras, membranes were probed for beta-actin and imaged again. All protein levels were normalized to becta-actin to control for potential protein loading differences.

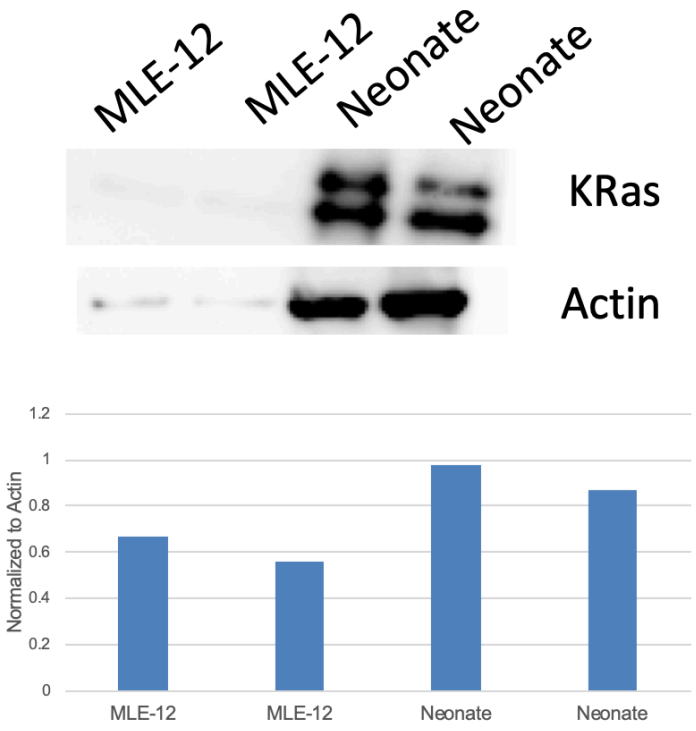

Figure 15: K-Ras expression in MLE-12 cell line and comparison to neonate E3 mouse lungs. Both iterations of MLE-12 and neonate are identical.

There is high expression of K-Ras in the neonate which makes the banding appear less clear; however, once I normalize to actin, expression of K-Ras in the MLE-12 cell line is actually quite high (approximately 0.6 in the MLE-12 cells and 0.95 in the neonate).

A pull-down assay is done in order to determine whether proteins are activated. The activated form of K-Ras is the GTP bound form and the inactivated form is when K-Ras is GDP bound. Before performing the pull-down assay, a specific western blot had to be run in order to determine optimal protein concentration to be used in the pull-down. A bovine serum albumin (BSA) protein quantification assay was performed and various amount of protein were placed on the gel.

Figure 16: Western blot showing KRas expression in MLE-12 cells where each lane represents different amounts of total loaded cell protein per lane. From left to right, the amounts of protein are: 20ug, 15ug, 4ug, 3ug, 2ug, 1.5ug.

The lane loaded with 4ug is the lowest amount of protein that can be used to produce a clear band via western blot. Due to the above data, the ideal amount of cell protein that was determined to be needed for the KRas pull-down assay was 400ug (100 x an amount that will give a clear band on a western blot).

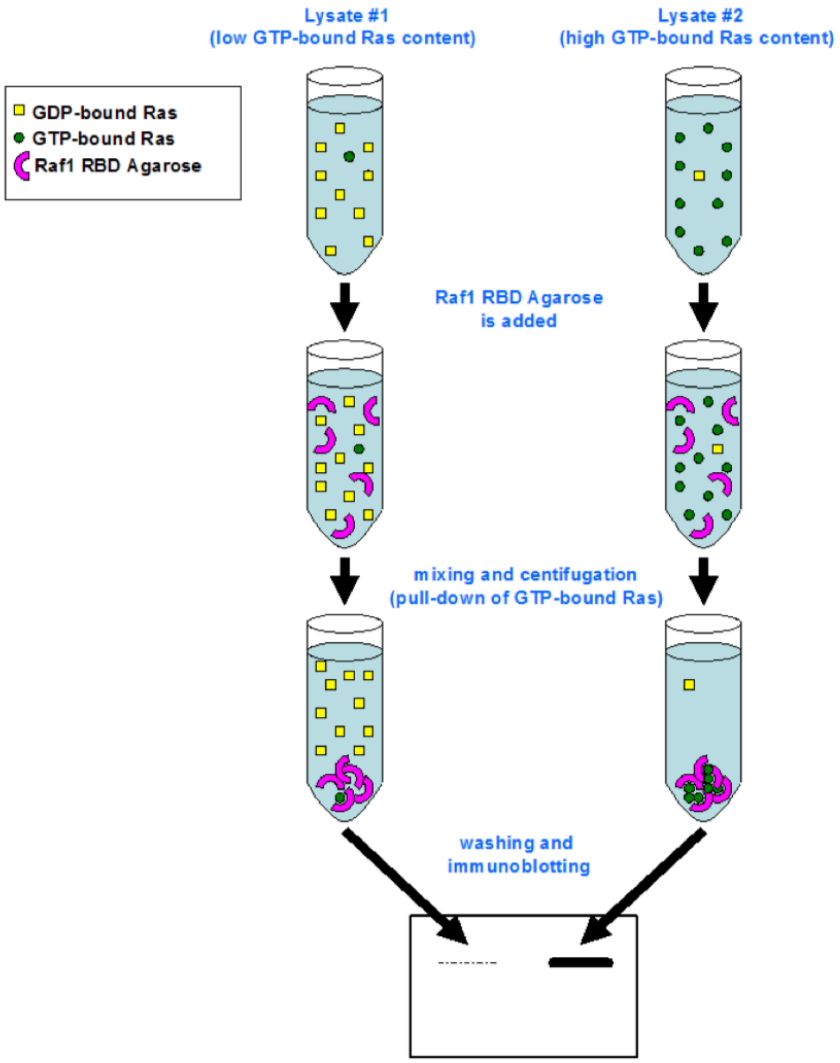

Figure 17: Schematic of KRas Pull-down Assay (from Cell BioLabs KRas Assay Protocol).

The KRas Pull-down was then performed using MLE12 whole cell lysates. GTP is used as a positive control because when K-Ras is GTP bound, this is the active form. Thus, adding extra GTP should activate K-Ras. Conversely, GDP is used as the negative control because when K-Ras is GDP bound, it is inactivated, and therefore,

should be undetectable via pull-down assay. GTP was loaded as a positive control and GDP was loaded as a negative control. Raf1-RBD agarose beads were used to conjugate and bind to activated KRas, the GTP-bound form. A portion of sample was taken prior to all parts of the pulldown assay for inputs as internal controls. All samples were loaded onto an SDS/polyacrylamide 10%-12% gradient gel, subjected to electrophoresis, and transferred to membranes for antibody probing which was detected using Femto.

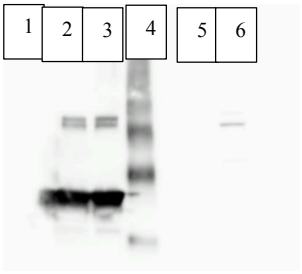

Figure 18: Sample Pull-down full blot. Lane 1 is the ladder, lane 2 is GTP, lane 3 is GDP, lane 4 is the positive control (provided by cell biolabs), lane 5 is another ladder, and lane 6 is the input.

The main issue with this blot and many similar to it, is that the bands were not in the correct molecular weight range, although the same bands had been present in previous KRas Western Blots. This suggested to me that KRas had several different isoforms; however, I should still be able to see a band at 21kDa, where it should be. In order to fix this, I cut the blot and overexposed the bottom half.

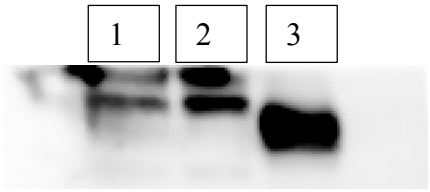

Figure 19: Pull-down blot cut and overexposed. Lane 1 is GTP (positive control), lane 2 is GDP (negative control), and lane 3 is positive internal control.

As seen in Figure 19, I was able to get a band with overexposure and cutting the blot, but not in the input.

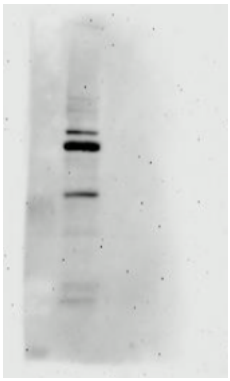

Figure 20: Pull-down blot cut and overexposed showing the input only.

Even with cutting and overexposing the input, I was unable to obtain a clear band in the correct molecular weight range and several additional bands were introduced. This also made me doubt the validity of the pull-down.

Another way I attempted to fix the some of the issues with the pull-down was by trying varying amounts of protein lysate.

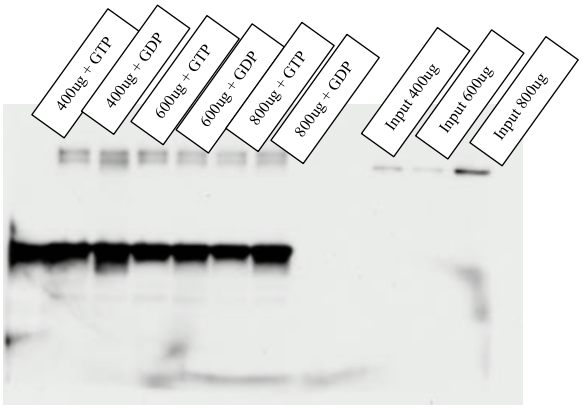

Figure 21: Pull-down with lane 1 loaded with 400ug of protein + GTP, lane 2 loaded with 400ug of protein + GDP, lane 3 loaded with 600ug of protein + GTP, lane 4 loaded with 600ug of protein + GDP, lane 5 loaded with 800ug of protein + GTP, and lane 6 loaded with 800ug of protein + GDP. Three lanes on the far right are inputs for 400ug, 600ug, and 800ug conditions.

Figure 21 shows that protein amount didn't make much of a difference in improving quality of pull-down.

Unfortunately, some problems were encountered with obtaining a negative control within the pull-down assay, as seen in figures 18 and 19. This may be due to the high amount of GTP present within the cells, that despite adding some GDP, it may not be sufficient for the KRas to become inactive. Next, I attempted to make sure that GTP was unavailable through two different methods: applying the chemical MPA (mycophenolic acid) or GDP flooding. MPA will deplete GTP and flooding the cell with GDP should kick out GTP due to concentration kinetics. For the experiment 1uM MPA was used. GDP flooding was done by increasing the concentration of GDP added by 100-fold. Neither method worked, and I was unable to obtain a proper

negative control, which rendered the assay invalid. There were additional challenges running the assay since the amount of lysate that would have been able to be collected from the strain device was much less than that required to properly run the assay.

2.4.3 Fluo-8 AM

Fluo-8 AM protocol was optimized for the MLE12 cell line. Fluo-8AM is a calcium sensitive dye that upon binding of intracellular calcium will increase its fluorescent signal. This was used to detect changes in intracellular calcium signaling that was hypothesized to occur during cellular stretch.

MLE12 cells were seeded into the PDMS cell chambers that were created by punching 6mm holes into PDMS and mounting onto glass coverslips to allow for better optical imaging. Cells were rinsed and dye was loaded in serum free, phenol-red free DMEM F12 with 0.02% pluronic acid. Fluo-8AM was incubated at 30^{o}C for 30 minutes on the cells. Cells were subsequently rinsed with Hank's Buffered Saline Solution (HBSS) and imaged in HBSS. MLE12 cells showed no baseline calcium signaling that could be detected with Fluo-8.

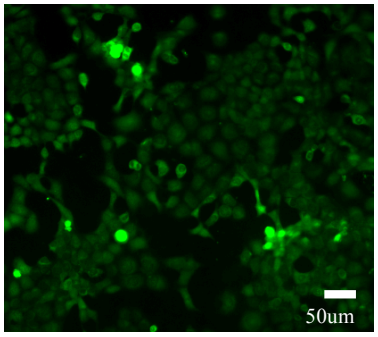

Figure 22: Sample Fluo-8AM image. MLE12 cells were incubated in Fluo-8AM dissolved in serum free, phenol-red free DMEM F12 with 0.02% pluronic acid for 30 minutes at 30 ^{o}C.

To validate that the lack of flux was not due to improper loading of Fluo-8AM, results were validated through comparison with a different cell, human pulmonary microendothelial cells (HPMECs). These cells did show baseline calcium flux.

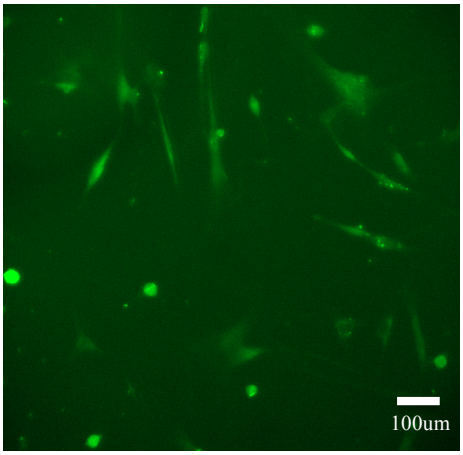

Figure 23: Sample Fluo-8AM image with HPMEC cells. Cells were incubated in Fluo-8AM dissolved in serum free, phenol-red free DMEM F12 with 0.02% pluronic acid for 30 minutes at 30 ^{o}C.

Additional validation that the Fluo-8 was properly loaded into the cells was done by using TRPV4 agonist GSK205. TRPV4 is a transmembrane calcum channel, and when cells are stimulated with GSK205, TRPV4 should be activated which would lead to a large spike in intracellular calcium. As anticipated, application of the agonist resulted in large calcium flux. Ionomycin, which raises intracellular calcium, was also tested and did not show significant effects in MLE12 cells, but did show substantial flux in HPMEC cells (figure 24).

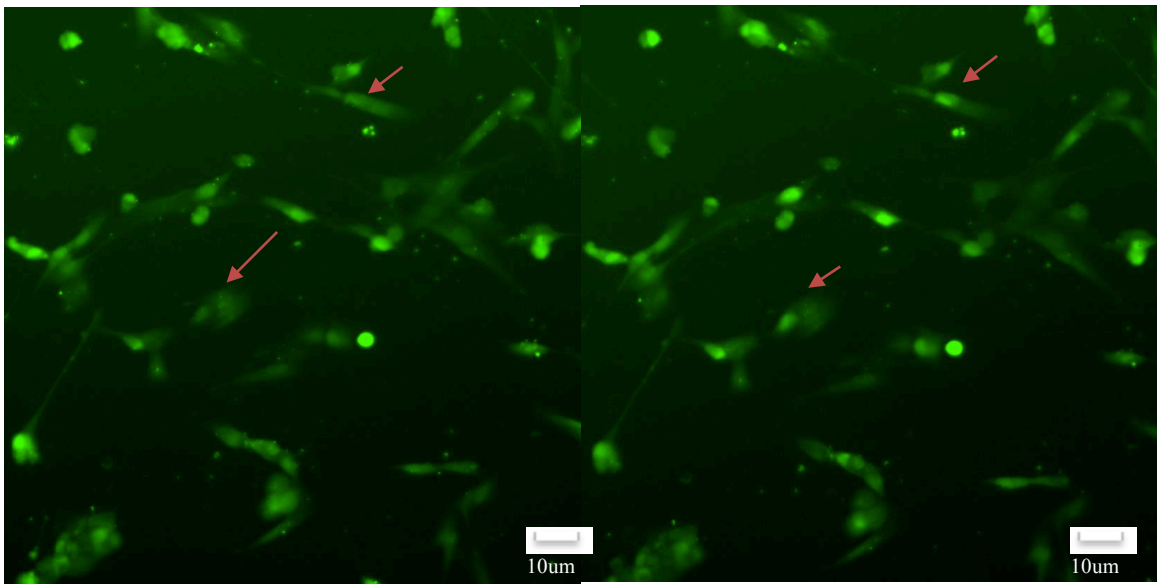

Figure 24: Sample Fluo-8AM image with HPMEC cells exposed to 5uM ionomycin. Arrows show areas where calcium changed from nuclear to cytoplasmic or vice versa.

Overall, these data indicate that Fluo-8AM is being taken up within the cells, but that MLE12 cells do not normally have calcium flux that is common in many other cell types. Since photobleaching made it difficult to image cells properly, imaging timepoints and intensity of laser were also optimized. Images were taken every 500ms with 20% intensity to avoid photobleaching.

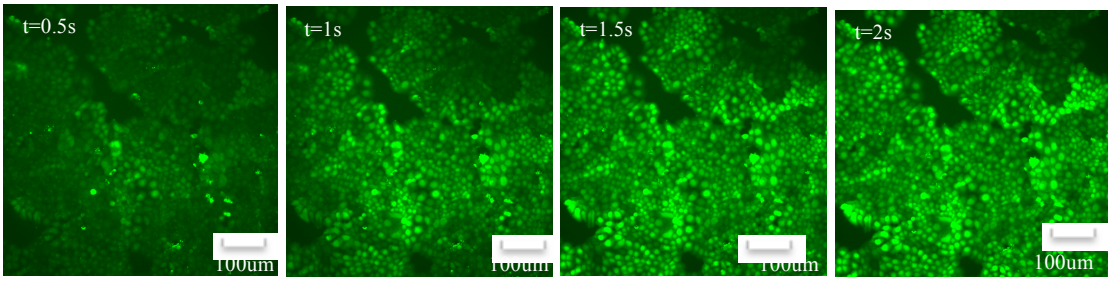

Figure 25: Propagation of calcium waves in response to GSK205 in MLE12 cells.

Chapter 3

RESULTS

3.1 Validation of Optical Clarity and PDMS Fabrication Consistency

I hypothesized that due to the qualities of the PDMS material, I would be able to obtain high quality images with immunofluorescent staining that were comparable to those achieved on a glass coverslip. Imaging through the acrylic base of the device did result in slightly lower quality images if the device was imaged during inflation. However, since the device could be removed post-stretch, stained, and imaged, this resulted in better image quality post-stretch.

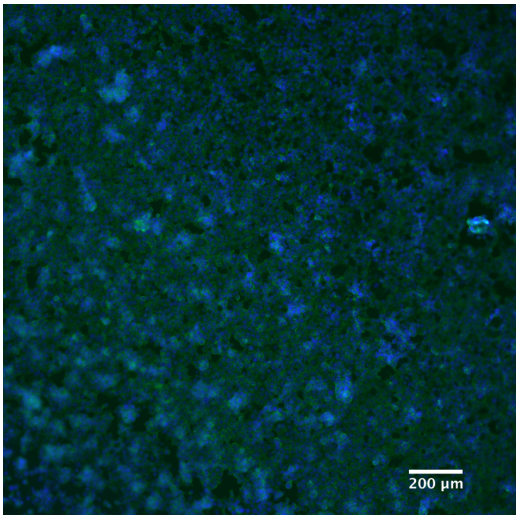

Figure 26: Immunofluorescent stain of MLE12 cells mounted on device for 24 hours and then stained with E-Cadherin and DAPI. Cells were imaged through the thin PDMS membrane.

3.2 Validation of PDMS Fabrication Consistency

I wanted to test that using the same parameters of membrane spinning each time would lead to identical membrane thickness regardless of length of coverslip. In order to validate that membranes were consistently the appropriate thickness after spinning, multiple membranes were tested and measured prior to mounting onto PDMS 6mm wells.

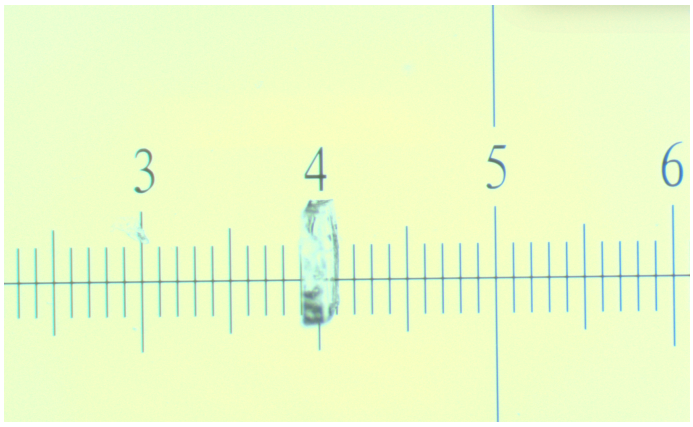

Figure 27: PDMS thickness measured using a calibration ruler. Each line represents 100um. Thickness is confirmed to be 100um.

3.3 Validation of Overall Fabrication Consistency

I wanted to test that due to the methods of manufacturing the device, I would be able to create identical iterations each time. PDMS was first made in a 1:20 ratio and poured into a 10cm petri dish. After curation, the PDMS block was removed and placed onto the acrylic top plate to use as a guide for punching the holes. A 6mm hole punch was used and a square was cut around the holes so that the device would fit on top of the acrylic pillars. Device dimensions were uniform. Plasma treatment was then used to attach each identical 100um membranes to the PDMS base.

3.4 Cell Lines

Another aim was to test that the MLE12 cell line in conjunction with Fluo-8 AM calcium dye could be used to measure calcium flux during stretch experiments. Unfortunately, since the dye has only transient efficacy, it photobleached off too quickly for proper data acquisition during a 3 hour stretch experiment. Thus, a new cell line was created using a lentiviral plasmid. The function of this plasmid was to visualize calmodulin activation and calcium flux in real time. This would work better than Fluo-8AM because it would not photobleach as easily and enable imaging over long periods of time (Fluo-8 has only transient effects that only last approximately one hour). The plasmid used was from Addgene, and expressed tdTomato GCamp6f-2A. GCamp is a fluorescent calcium indicator. It works by containing calcium binding motifs and can show calcium flux within the cells. Cells were infected with lentivirus to create a permanent expression of the transgene. There was no selection marker within the plasmid but tdTomato could be used to identify cells that were positive for expression. The two fluorophores in the plasmid enabled proper identification of cells that were expressing the plasmid.

3.4.1 Semi-Clonal Selection

The original cell line had approximately 40% of cells expressing the marker, which is not high enough expression to obtain proper data during my experiment. Without a chemical selection marker, I needed to create a different method of shifting to a higher expressing population to ensure a high enough number of cells were expressing the plasmid to be useful during my experiments. Thus, a selection process was done by plating a low density of cells within a 96-well plate. I then checked each

well for tdTomato signal, and replated wells with the highest amount of expression. This resulted in a semi-clonal cell line with approximately 70%-80% expression.

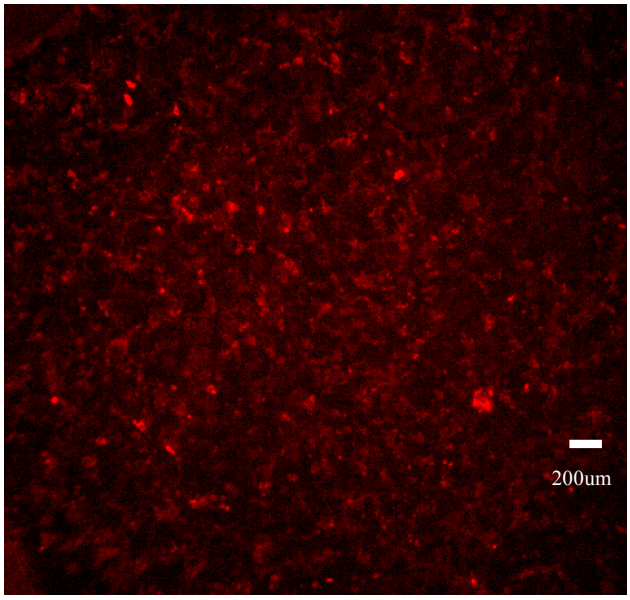

Figure 28: MLE12 tdTomato GCamp6F cells seeded on PDMS membrane for 24 hours after completion of clonal selection. Cells are imaged at 5x through acrylic device.

3.5 Seeding Technique

I hypothesized that due to the properties of PDMS, this would pose a challenge to cell adherence and that a coating would be required in order for cells to grow properly on PDMS. Thus, I tried different ECM coatings to see what worked best to promote cell adherence. I tried fibronectin because it could promote cell adhesion by binding to integrins. I tried PEI (polyethylenimine) because it is a cationic polymer which could work by attracting the negative charge of the cells.

Table 1: Coatings and Conditions Attempted for Promoting Cell Growth on PDMS.

Type of Coating/Condition	Percent Adherence after 24 Hours in Culture
2% PEI for 90 minutes + 50 mg/mL Fibronectin for 60 minutes	75%
2% PEI for 90 minutes only	40%
50mg/mL Fibronectin for 60 minutes only	95%

Thus, the coating selected was 50mg/mL fibronectin for 60 minutes. Fibronectin was diluted in PBS without calcium and magnesium and incubated at 30^{o}C. Following treatment, fibronectin was rinsed with PBS and cells were then seeded.

3.6 Validation of Stretch Conditions

3.6.1 Using Fluorescent Markers to Visualize and Track Strain

I wanted to test whether dragon green beads could be used to track membrane deformation and calculate strain. In order to test consistency of stretch, dragon green beads were incorporated into the fabrication of the PDMS membrane and mounted onto the PDMS base. This could then be imaged during stretch to track the deformation of the membrane.

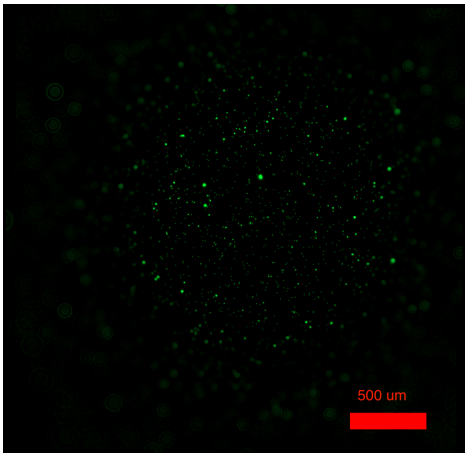

Figure 29: Dragon Green beads on 10um PDMS membrane for device calibration. Imaged at 5x through the acrylic base of the device.

3.7 Proliferation Data

I hypothesized that proliferation would increase with the application of strain on MLE12 cells. I hypothesized that control wells would have the least number of proliferating cells, low strain wells would have an intermediate amount of proliferating cells, and high strain wells would have the highest amount of proliferation.

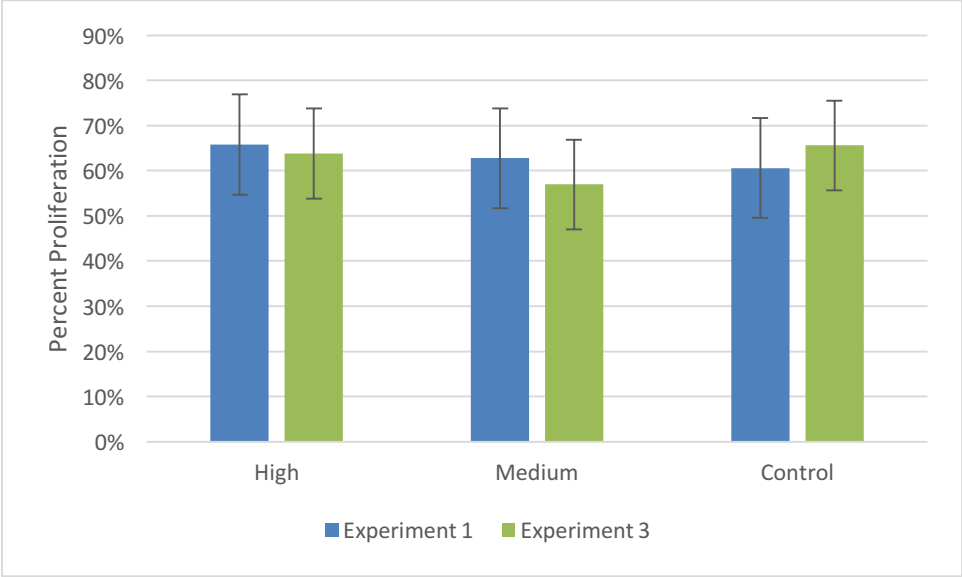

Figure 30: Average proliferation (%) for high, medium and control strains. Three different experiments are shown.

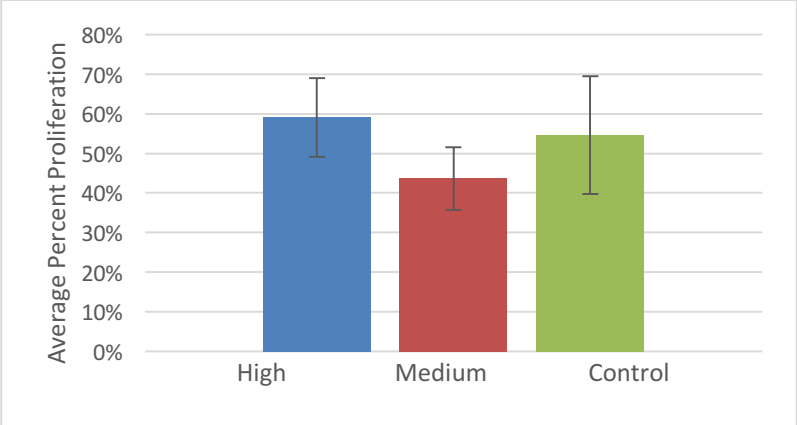

Figure 31: Average proliferation (%) across all the experiments.

The data did not show the hypothesized trend. There was high variability between data points and although the high strain pillar did result in the most proliferation, the

medium pillar had slightly less proliferation than the control. The values were also fairly close together and not significant ($p>0.05$).

3.8 GCaMP Data

I hypothesized that GCaMP activation would increase with the application of strain on MLE12 cells, based on previous studies that have shown increased branching due to calcium release and correlation between calcium release and peristaltic contractions. I hypothesized that control wells would have the least amount of fluorescence, low strain wells would have an intermediate amount of fluorescence, and high strain wells would have the highest amount of fluorescence.

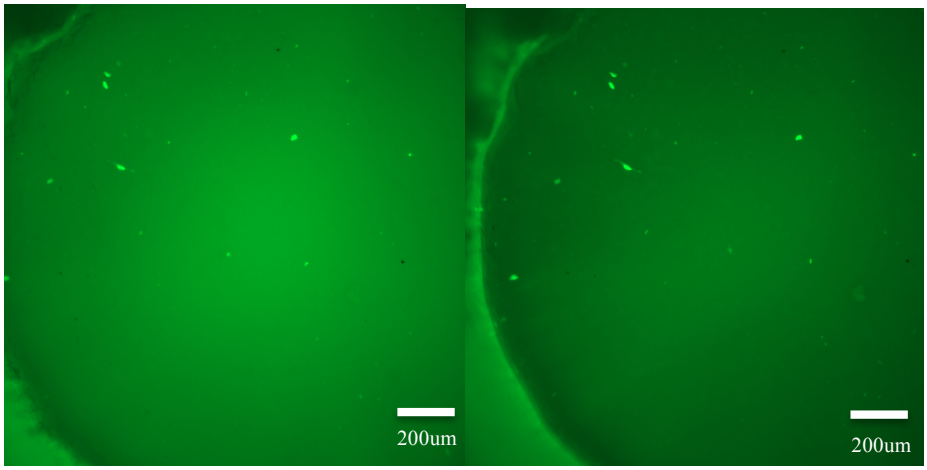

Figure 32: High strain pillar A imaged before strain and after strain.

Due to decreasing background fluorescence it was difficult to tell if fluorescence of the individual cells increased or not. Thus, the amount of calcium release could not be determined.

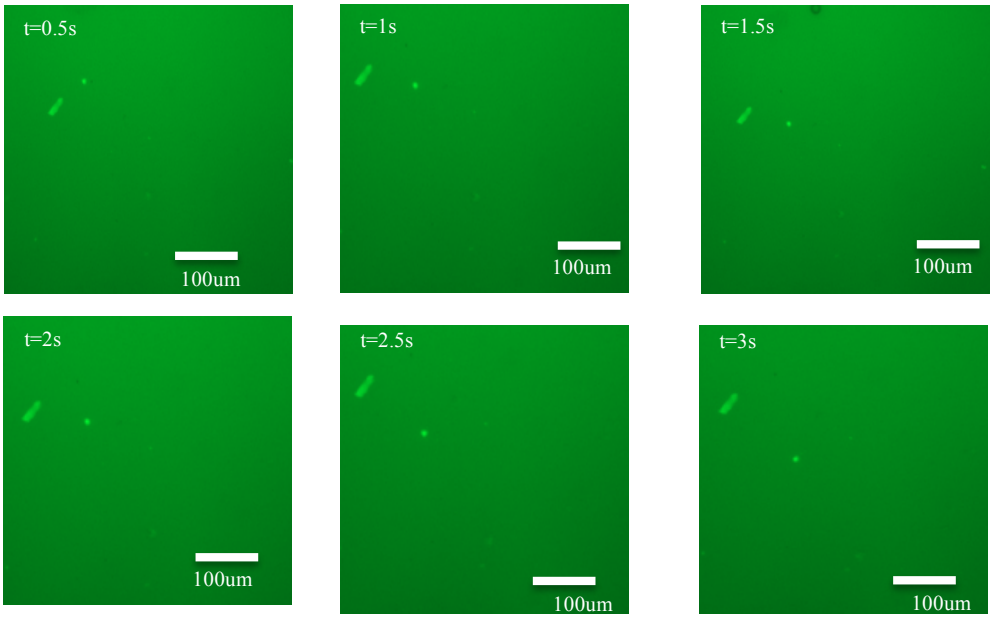

Figure 33: High strain pillar B imaged during strain. Position of fluorescent signal changes in the various frames.

A pattern of GCamp activation like that of figure 35 could be expected in future experiments, where calcium signal propagates between cells.

Chapter 4

DISCUSSION

The methods developed in this study enable study of mechanotransduction and can be applied to multiple organ systems. The design of the device was created to facilitate imaging. Development of imaging techniques such as mounting membranes onto coverslips also improved image quality and enabled acquisition of images at higher magnification. Fabrication of the device was then validated in various different ways. As seen in Figure 21, PDMS thickness was confirmed to be consistently 10um thick. All other dimensions of the PDMS device were also checked for consistency. The GCamp cell line was validated using the tdTomato marker and clonal selection. The semi-clonal population was confirmed to have the same characteristics of the original cell line. Various methods were tested for cell adherence onto PDMS and overall, 50mg/mL of fibronectin promoted the most adherence (approximately 95%). This is in line with my hypothesis that a coating would be required for cell adherence since PDMS does not traditionally allow for cell adherence.

The proliferation data from the device experiments deviated a bit from the hypothesized trends. No clear trend in proliferation was found, although I was expecting to see higher proliferation in the high strain pillars, less proliferation in the low strain pillars and the least amount of proliferation in the control pillars. I would have expected this because numerous other studies have shown increased proliferation with the application of stretch in several different organ systems[28,29,30,31]. The lack of consistency in proliferation data may have been due to inconsistencies within the device that are apparent in its calibration. However, the proliferation studies served as a good first step in measuring the effects of strain on the cells. The GCamp data also

failed to show a clear trend in terms of fluorescence measurements. This may have been due to evaporation of the liquid as the experiment progressed. This would have led to less background fluorescence, and thus less overall fluorescence despite any potential changes in cellular fluorescence and GCamp signaling. A different method of covering the device had to be developed in order to avoid liquid evaporation. Although the proposed model did have some limitations, it will provide guidance in future studies involving the effects of stretch on various organ systems.

Chapter 5

CONCLUSION AND FUTURE DIRECTIONS

This study proposes a mechanotransduction signaling pathway in mouse lung epithelial cells and provides a method for testing the effects of controlled pressure on cells. The signaling pathway proposed involves TRPV4 activation, calcium release, calmodulin activation, Ras-GRF activation, and K-Ras activation. To test TRPV4 activation and calcium release, a GCamp cell line was created and Fluo-8AM protocols were optimized. For K-Ras activation testing, pull-down assay optimization was commenced. A novel device was created with an acrylic base and PDMS piece for cell seeding. Optical clarity for imaging was achieved. Protocols were created for spinning 100um PDMS membranes, mounting membranes onto PDMS bases, and seeding cells onto PDMS.

Proliferation experiments deviated from expected trends based on previous studies[28,29,30,31]. Variations in the data could be due to some of the inconsistencies in strain applied to each pillar by the device. This can likely be fixed with a circular conformation of the device. GCamp data was somewhat inconclusive due to evaporation and decrease of background fluorescence. However, potential signaling was identified and could be used to guide future work.

For future directions, I would like to create a new device that is much larger so that I can easily extract enough protein for pull-down assays. I would make a device that has pillars oriented in a round configuration so as to ensure perfect symmetry and equal distance between pillars and vacuum ports. A version of this is already being tested in our lab and preliminary data shows that this configuration would give equibiaxial strain. I would also like to automate the process of fabrication of the

device instead of hand-cutting it with a laser. In order to streamline the process of device manufacturing I could 3D print molds that will ensure perfect placement of holes in the back of the device each time. Thus, different iterations of the device could be more consistent with each other.

If a larger device with equibiaxial strain pillars is achieved, and it is possible to obtain approximately 400ug of protein lysate, then K-Ras pull-downs can be attempted. The first step after calibration of the new device would be to use the EdU kit to test for proliferation. This was the most reliable assay and the best way to test the overall effects of stretch. Using proliferation, one could test whether stretch conditions are adequate and make adjustments where needed. Then, either Fluo-8AM or the GCamp cell line to test calcium flux in relation to stretch. Fluo-8AM should be loaded as described in the methods section of this thesis. Fluo-8AM could be loaded at the end of stretch to collect the last 45 minutes-1 hour of calcium stretch data. Continuous imaging would not be possible because the dye has only transient effects. If continuous imaging is desired, the GCamp cell line can be used. If a larger iteration of the device is achieved, and at least 400ug of protein lysate can be obtained, the next step could be to test KRas activation using a pulldown assay. Different beads would be needed, since the Cell BioLabs Kit is unreliable. GTP and GDP and most other kit components can be obtained separately. First, the western blot should be performed and then the Pull-Down can proceed once a clear band is obtained from the western lysate. If the band is faint, more protein may be needed or a different antibody can be tested. The Proteintech KRas antibody I used worked well.

In the next set of experiments, GSK101 could be used as a TRPV4 agonist and GSK201 could be used as a TRPV4 antagonist. TRPV4 shRNA could also be used to

confirm these effects. Then, I would focus on calcium/calmodulin and could use a calcium agonist, Calp-3 and a calcium antagonist W-7, as well as CaM shRNA. RasGRF could be knocked out with shRNA, and K-Ras could be targeted using salirasib and tipifarnib (antagonists). The same assays could be used to test for various parameters of the pathway. Stretch conditions could also be altered and tested. Medium strain with the same parameters described in this study could be used, as well as higher strains with a 12mmHg vacuum and lower strains of 4mmHg vacuum. Different frequencies and duration of strain can also be tested with the current system. The development of this insight will enable us to gain a greater understanding of lung development as well as the stretch-related development of many organs.

REFERENCES

1. Jesudason EC, Connell MG, Fernig DG, Lloyd DA, Losty PD. Early lung malformations in congenital diaphragmatic hernia. *J Pediatr Surg* 2000; 35: 124–127.

2. About Congenital Diaphragmatic Hernia (CDH). https://www.ssmhealth.com/cardinal-glennon/fetal-care-institute/lungs/congenital-diaphragmatic-hernia-(cdh)/about.

3. Cilley R., Zgleszewski S., and Chinoy M. Fetal lung development: airway pressure enhances the expression of developmental genes. NCBI.

4. Nelson, C. M., Gleghorn, J. P., Pang, M. F., Jaslove, J., Goodwin, K., Varner, V. D., ... & Stone, H. A. (2017). Microfluidic chest cavities reveal that transmural pressure controls the rate of lung development. Development, dev-154823.

5. Jesudason EC et al., Peristalsis of airway smooth muscle is developmentally regulated and uncoupled from hypoplastic lung growth. *Am J Physiol Lung Cell Mol Physiol* 291: L559 –L565, 2006.

6. Liu, M., Xu, J., Souza, P., Tanswell, B., Tanswell, A. K., & Post, M. (1995). The effect of mechanical strain on fetal rat lung cell proliferation: comparison of two-and three-dimensional culture systems. *In Vitro Cellular & Developmental Biology-Animal*, *31*(11), 858-866.

7. Rhodes, J., Saxena, D., Zhang, G., Gittes, G. K., & Potoka, D. A. (2015). Defective parasympathetic innervation is associated with airway branching abnormalities in experimental CDH. *American Journal of Physiology-Heart and Circulatory Physiology*.

8. Burri, P. H. (1984). Fetal and postnatal development of the lung. *Annual review of physiology*, *46*(1), 617-628.

9. Warburton, D., El-Hashash, A., Carraro, G., Tiozzo, C., Sala, F., Rogers, O., De Langhe, S., Kemp, P. J., Riccardi, D., Torday, J., et al. (2010). Lung organogenesis. *Curr Top Dev Biol* 90, 73-158.

10. Featherstone NC, Jesudason EC, Connell MG, Fernig DG, Wray S, Losty PD, and Burdyga TV**.** Spontaneous propagating calcium waves underpin airway peristalsis in embryonic rat lung. *Am J Respir Cell Mol Biol* 33: 153–160, 2005.

11. Jesudason, E. C. (2009). Airway smooth muscle: an architect of the lung?. *Thorax*, *64*(6), 541-545.

12. Nayak, P. S., Wang, Y., Najrana, T., Priolo, L. M., Rios, M., Shaw, S. K., & Sanchez-Esteban, J. (2015). Mechanotransduction via TRPV4 regulates inflammation and differentiation in fetal mouse distal lung epithelial cells. *Respiratory research*, *16*(1), 60.

13. Morgan, J. T., Stewart, W. G., McKee, R. A., & Gleghorn, J. P. (2018). The Mechanosensitive Ion Channel TRPV4 is a Regulator of Lung Development and Pulmonary Vasculature Stabilization. *Cellular and molecular bioengineering*, *11*(5), 309-320.

14. Brennan, S. C., Finney, B. A., Lazarou, M., Rosser, A. E., Scherf, C., Adriaensen, D., ... & Riccardi, D. (2013). Fetal calcium regulates branching morphogenesis in the developing human and mouse lung: involvement of voltage-gated calcium channels. *PloS one*, *8*(11), e80294.

15. Johnson, L., Greenbaum, D., Cichowski, K., Mercer, K., Murphy, E., Schmitt, E., ... & Jacks, T. (1997). K-ras is an essential gene in the mouse with partial functional overlap with N-ras. *Genes & development*, *11*(19), 2468-2481.

16. Ustiyan, V., Zhang, Y., Perl, A. K. T., Whitsett, J. A., Kalin, T. V., & Kalinichenko, V. V. (2016). β-catenin and Kras/Foxm1 signaling pathway are critical to restrict Sox9 in basal cells during pulmonary branching morphogenesis. *Developmental Dynamics*, *245*(5), 590-604.

17. Cardoso, W. V., & Lü, J. (2006). Regulation of early lung morphogenesis: questions, facts and controversies. *Development*, *133*(9), 1611-1624.

18. Morrisey, E. E. (2013). Balancing the developmental niches within the lung. *Proceedings of the National Academy of Sciences*, *110*(45), 18029-18030.

19. Chang, D. R., Alanis, D. M., Miller, R. K., Ji, H., Akiyama, H., McCrea, P. D., & Chen, J. (2013). Lung epithelial branching program antagonizes alveolar differentiation. *Proceedings of the National Academy of Sciences*, *110*(45), 18042-18051.

20. Shaw, A. T., Meissner, A., Dowdle, J. A., Crowley, D., Magendantz, M., Ouyang, C., ... & Stone, J. R. (2007). Sprouty-2 regulates oncogenic K-ras in lung development and tumorigenesis. *Genes & development*, *21*(6), 694-707.

21. Gudermann, T., & Roelle, S. (2006). Calcium-dependent growth regulation of small cell lung cancer cells by neuropeptides. *Endocrine-related cancer*, *13*(4), 1069-1084.

22. Fam, N. P., Fan, W. T., Wang, Z., Zhang, L. J., Chen, H., & Moran, M. F. (1997). Cloning and characterization of Ras-GRF2, a novel guanine nucleotide exchange factor for Ras. *Molecular and Cellular Biology*, *17*(3), 1396-1406.

23. Chen, L., Zhang, L. J., Greer, P., Tung, P. S., & Moran, M. F. (1993). A murine CDC25/ras-GRF-related protein implicated in ras regulation. *Developmental genetics*, *14*(5), 339-346.

24. Freshney, N. W., Goonesekera, S. D., & Feig, L. A. (1997). Activation of the exchange factor Ras-GRF by calcium requires an intact Dbl homology domain. *FEBS letters*, *407*(1), 111-115

25. Rossman, K. L., Der, C. J., & Sondek, J. (2005). GEF means go: turning on RHO GTPases with guanine nucleotide-exchange factors. *Nature reviews Molecular cell biology*, *6*(2), 167.

26. Pugin, J., Dunn-Siegrist, I., Dufour, J., Tissieres, P., Charles, P. E., & Comte, R. (2008). Cyclic stretch of human lung cells induces an acidification and promotes bacterial growth. *American journal of respiratory cell and molecular biology*, *38*(3), 362-370.

27. Rentzsch, I., Santos, C. L., Huhle, R., Ferreira, J. M., Koch, T., Schnabel, C., ... & de Abreu, M. G. (2017). Variable stretch reduces the pro-inflammatory response of alveolar epithelial cells. *PloS one*, *12*(8), e0182369.

28. Felsen, D., Diaz, B. J., Chen, J., Gonzalez, J., Kristensen, M. L. V., Bohn, A. B., ... & Nørregaard, R. (2017). Pressure and stretch differentially affect proliferation of renal proximal tubular cells. *Physiological reports*, *5*(17).

29. Dai, Y., Tian, Y., Luo, D. Y., Wazir, R., Yue, X., Li, H., & Wang, K. J. (2015). Cyclic stretch induces human bladder smooth muscle cell proliferation in vitro through muscarinic receptors. *Molecular medicine reports*, *11*(3), 2292-2298.

30. Banerjee, I., Carrion, K., Serrano, R., Dyo, J., Sasik, R., Lund, S., ... & Chen, J. (2015). Cyclic stretch of embryonic cardiomyocytes increases proliferation, growth, and expression while repressing Tgf-β signaling. *Journal of molecular and cellular cardiology*, *79*, 133-144.

31. Hegarty, P. K., Watson, R. W. G., Coffey, R. N., Webber, M. M., & Fitzpatrick, J. M. (2002). Effects of cyclic stretch on prostatic cells in culture. *The Journal of urology*, *168*(5), 2291-2295.

32. Wirtz, H. R., & Dobbs, L. G. (1990). Calcium mobilization and exocytosis after one mechanical stretch of lung epithelial cells. *Science*, *250*(4985), 1266-1269.

Appendix A

PROLIFERATION DATA